

## ELASTIC AND INELASTIC WIDE-COLUMN MODELS FOR RC NON-RECTANGULAR WALLS

K. Beyer<sup>1</sup>, A. Dazio<sup>1</sup> and M.J.N. Priestley<sup>2</sup>

<sup>1</sup> *Institute of Structural Engineering, ETH Zurich, Switzerland*

<sup>2</sup> *European School for Advanced Studies in Reduction of Seismic Risk (ROSE School), Pavia, Italy*  
*Email: beyer@ibk.baug.ethz.ch, dazio@ibk.baug.ethz.ch*

### ABSTRACT :

Wide-column models (WCM) are frequently used in the seismic analysis of non-rectangular reinforced concrete (RC) walls which respond in the inelastic range. Guidelines in the literature on the application of WCMs to non-rectangular walls are almost exclusively based on studies of elastic systems which shear deformations are relatively small when compared to flexural deformations. From own large-scale quasi-static cyclic tests of U-shaped RC walls it was found that depending on the direction of loading the shear displacement constitute a significant part to the total displacements. This paper shows that if the existing modeling recommendations for WCMs are extended to either elastic or inelastic systems with relatively large shear flexibilities, the stiffness of the system is overestimated. New modeling recommendations, in particular for the properties of the horizontal links in WCMs are formulated. Analysis results of WCMs with revised properties are compared against results obtained from analysis of elastic shell models, inelastic macro elements and experimental evidence.

**KEYWORDS:** Reinforced concrete, structural walls, U-shaped walls, numerical simulations, large-scale tests, quasi-static cyclic tests.

### 1. INTRODUCTION

Although non-rectangular walls, such as for example U-shaped walls or core walls of more complicated shape, are frequently used in reinforced concrete (RC) buildings, experimental and numerical studies on their seismic behavior are relatively scarce. In an experimental program at the ETH Zurich two U-shaped walls were tested under quasi-static cyclic loading. The results of these tests were used in a numerical study which objective was to evaluate the suitability of relatively simple analysis tools for the seismic analysis of core walls. The modeling approaches that were selected for this study are the wide-column analogy and a macro-element modeling approach using the program PERFORM (CSI, 2007). Both analysis tools are widely used in engineering practice when entire RC buildings are analyzed for seismic loading.

This paper presents the findings of the numerical studies and highlights the points that require particular attention when modeling the walls. Since the numerical results are compared against the experimental evidence gained from the quasi-static cyclic tests a brief summary of the tests is given in Section 2. However, this section will only contain the information which is required for the reader to follow the presentation of the numerical results in Section 3 and 4 since a detailed description of the tests has been given elsewhere (Beyer *et al.*, 2008a). The paper concludes with a summary of the findings and modeling recommendations (Section 5).

### 2. QUASI-STATIC CYCLIC TESTS ON U-SHAPED WALLS

Two U-shaped walls built at half-scale were tested under a quasi-static cyclic loading regime at the structural engineering laboratories of the ETH in Zurich. The cross sections of the two test units differed mainly regarding their wall thickness: Test unit A (TUA) had a wall thickness of 0.15m and Test Unit B (TUB) a wall thickness of 0.10m which correspond at full-scale to wall thicknesses of 0.30m and 0.20m, respectively. Both walls were capacity-designed and subjected to a constant axial load during testing. The cross section of the test units and a summary of the wall dimensions, axial load ratios and reinforcement ratios are given in Table 1. Also included in Table 1 is the data of a U-shaped wall that was tested under quasi-static cyclic loading at the research centre

in Ispra (Pégon *et al.*, 2000). As part of that research program three specimens of a single U-shaped wall configuration were tested under different directions of loading. The test units were characterized by a rather compact section which had been designed for medium ductility according to a draft of Eurocode 8 (CEN, 1994). The objective of the ETH-tests was to complement the work carried out in Ispra by testing walls that were less compact and designed for high ductility. Unlike in the case of the Ispra-tests no particular code was followed when designing the test units but design principles were applied which were judged reasonable without being overly conservative with respect to the shear and sliding shear design.

The setup for the ETH-tests is shown in Fig. 1a. Three actuators were used to control the movement of the wall head: the EW-actuator which loaded the web and the two NS-actuators which loaded the flanges (Fig. 1c). They were connected to the “collar” at the top of the wall which had an increased wall thickness of 300mm for both

Table 1 U-shaped walls: Comparison of cross sections of TUA, TUB and the units tested in Ispra.

	TUA	TUB	Ispra
Scale	1:2	1:2	1:1
Shear span $M/V$	2.95m <sup>1)</sup> / 3.35m <sup>2)</sup>	2.95m <sup>1)</sup> / 3.35m <sup>2)</sup>	3.90m <sup>1,2)</sup>
Shear span ratio $h/l_w$	2.81 <sup>1)</sup> / 2.58 <sup>2)</sup>	2.81 <sup>1)</sup> / 2.58 <sup>2)</sup>	3.12 <sup>1)</sup> / 2.60 <sup>2)</sup>
Axial load / Axial load ratio <sup>3)</sup>	780kN / 0.02	780kN / 0.04	2120kN / 0.10-0.12
Compactness ratios:			
$t_w/l_{web} / t_w/l_f$	0.12 / 0.14	0.08 / 0.10	0.17 / 0.20
Vertical reinforcement ratio:			
$\rho_{tot}$	0.71%	1.01%	0.56%
Horizontal reinforcement ratio:			
$\rho_{h, web} / \rho_{h, flange}$	0.30% / 0.30%	0.45% / 0.45%	0.54% / 0.32%

<sup>1)</sup> NS direction (parallel to the flanges); <sup>2)</sup> EW direction (parallel to the web); <sup>3)</sup> at the wall base.

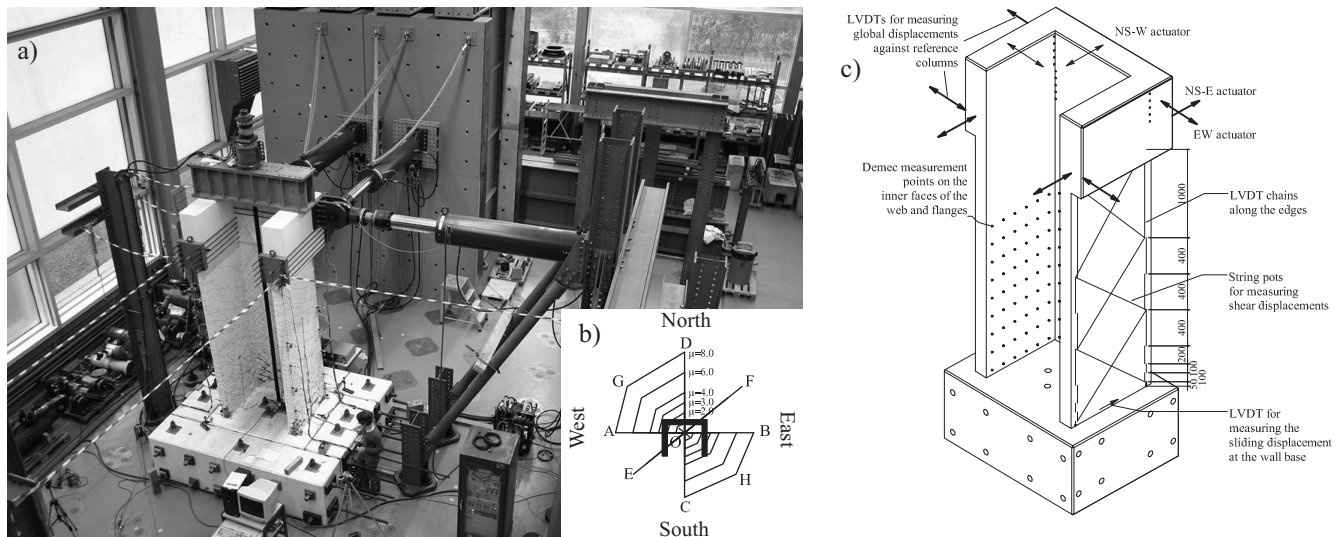


Figure 1 Quasi-static cyclic tests on U-shaped walls at the ETH: Photo of the test setup (a), bi-directional loading history (b) and instrumentation of the test units (c).

TUA and TUB. The applied loading history was a bi-directional loading history (Fig. 1b) which comprised at each ductility level a cycle parallel to the web ( $O \rightarrow A \rightarrow B \rightarrow O$ ), a cycle parallel to the flanges ( $O \rightarrow C \rightarrow D \rightarrow O$ ), a cycle in diagonal direction ( $O \rightarrow E \rightarrow F \rightarrow O$ ) and a “sweep” ( $O \rightarrow A \rightarrow G \rightarrow D \rightarrow C \rightarrow H \rightarrow O$ ). During these cycles the rotation of the wall head was restrained by the two actuators loading the flanges (actuators NS-E and NS-W). The load pattern was repeated at displacement ductilities of  $\mu_{\Delta}=1, 2, 3, 4, 6$  and  $8$  until failure occurred. Prior to nominal yield a slightly different load pattern was applied which only consisted of cycles in EW, NS, and diagonal direction.

During testing, the load-deformation behavior of the test unit was monitored by a large number of instruments. Apart from the applied forces and the global displacements at the wall head, the elongation along the four outer edges, the shear deformations, the sliding displacements at the wall base and strains of the shear reinforcing bars were measured with hard-wired instruments. In addition, manual measurements were taken at peak and zero load positions. They comprised Demec measurements on the inside faces of the web and flanges and crack width measurements of selected cracks. An overview of the applied instrumentation is shown Fig. 1c. The global force-displacement hysteresis curves will be shown in Section 3 and 4 where the analysis results are compared to the experimental evidence. The main finding from the evaluation of the local deformations concerned the shear deformations: Like for rectangular capacity-designed walls the ratio of shear to flexural deformations ( $\Delta_s/\Delta_f$ ) remained approximately constant as the inelastic displacement demand on the walls increased. However, the  $\Delta_s/\Delta_f$ -ratio varied considerably between the web and flanges and also for different directions of loading. Moreover, for some directions of loading, the  $\Delta_s/\Delta_f$ -ratios were considerably larger ( $\Delta_s/\Delta_f$  up to 0.53 and 0.72 for TUA and TUB, respectively) than typical ratios of rectangular walls subjected. A detailed summary of the results can be found in Beyer *et al.* (2008a).

### 3. WIDE-COLUMN MODELS OF THE U-SHAPED WALLS

The wide-column analogy was originally developed for planar wall structures such as walls with openings (e.g. Clough *et al.*, 1964) and was later extended to non-planar structures (e.g. MacLeod and Hosny, 1977). Despite being widely applied for seismic analysis of structures, only very little literature on wide-column models (WCMs) with inelastic properties has been found. Most of the research carried out in the past concentrated on the behavior of WCMs with elastic properties and on eliminating any disadvantages related to the discretization of the walls into beam elements. The objective of this section is to give a brief description of the WCM for TUA and a summary of the insight gained during the modeling process. Due to space limitations the analysis of TUB and the sensitivity of the model to different modeling assumptions will not be discussed but the interested reader is referred to Beyer *et al.* (2008b) for a detailed documentation of the study.

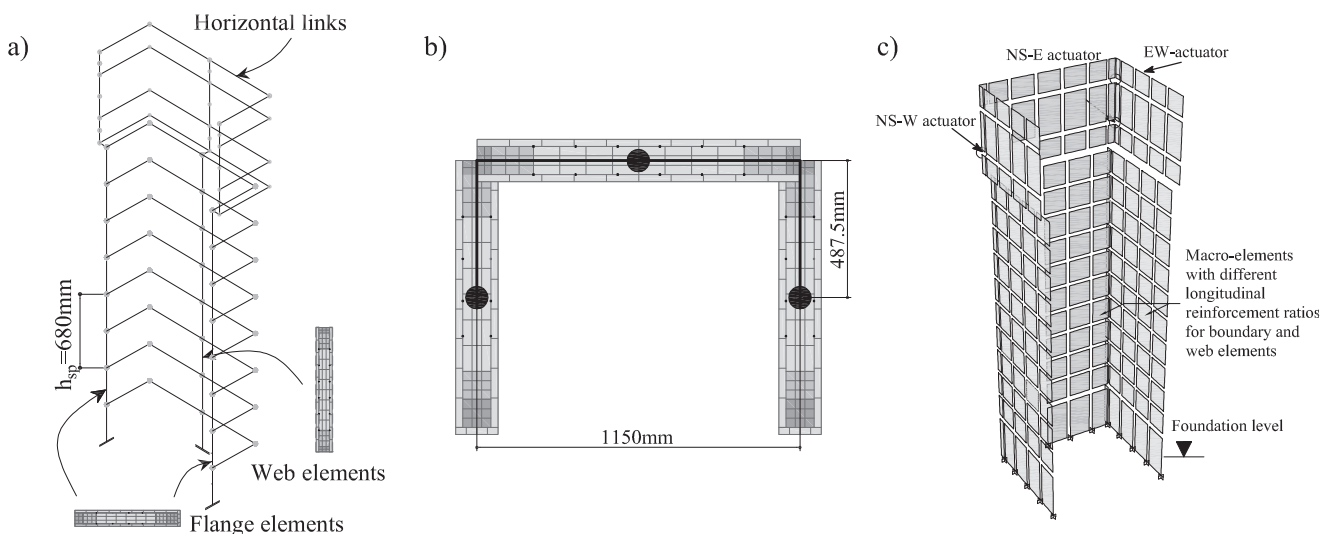


Figure 2 Numerical models of TUA: Isometric view of the WCM (a), subdivision of the cross section of the WCM into fiber elements showing also the position of the wall elements and the wall links (b), and the PERFORM model of TUA (c).

In the study presented here the research program “Opensees” (Mazzoni *et al.*, 2006) was used for the analysis of the WCM of TUA. The program was chosen at the onset of the study because it offers a large flexibility and a wide-range of elements and hysteretic rules. However, the WCM presented here uses only standard element types and material models and therefore commercial software packages such as e.g. SAP2000 (CSI, 2006) or Seismostruct (Seismosoft, 2007) could also be employed for the analysis. Figure 2a shows the WCM of TUA. The vertical elements represent the web and flanges and were non-linear displacement based beam elements with fiber sections (Fig. 2b) defining the flexural and axial properties. The displacement-based elements in Opensees have no shear flexibility and therefore zero-length shear springs were introduced at the nodes at midheight between the horizontal links to model the shear flexibility. In a first model (“reference model”) the spring properties were computed to represent the shear stiffness of uncracked concrete sections assuming a shear area of  $A_{s0}=0.8A_{gross}$ . This is a very crude assumption and grossly overestimates the actual shear stiffness for deformations in the inelastic range. The shear stiffness of capacity-designed walls is directly related to the flexural deformations (Vallenas *et al.*, 1979; Oesterle *et al.*, 1984; Dazio, 2000; Beyer *et al.*, 2008b) and therefore decreases as the displacement demand on the structure increases. However, since most structural analysis programs do not allow for an interaction of the shear and flexural stiffnesses nor allow updating the shear stiffness during the analysis process, it is necessary to use an average shear stiffness. In the second model (“updated model”) the shear stiffness was computed for  $\mu_{\Delta}=4.0$  from experimentally determined  $\Delta_s/\Delta_f$ -ratios for loading in the principal directions (EW and NS direction).

In the literature (Avramidis, 1991; Reynouard and Fardis, 2001) it is recommended to model the horizontal links connecting the vertical elements as rigid apart from the torsional stiffness; for the latter a value of  $GK=Gh_{sp}t_w^3/3$  is

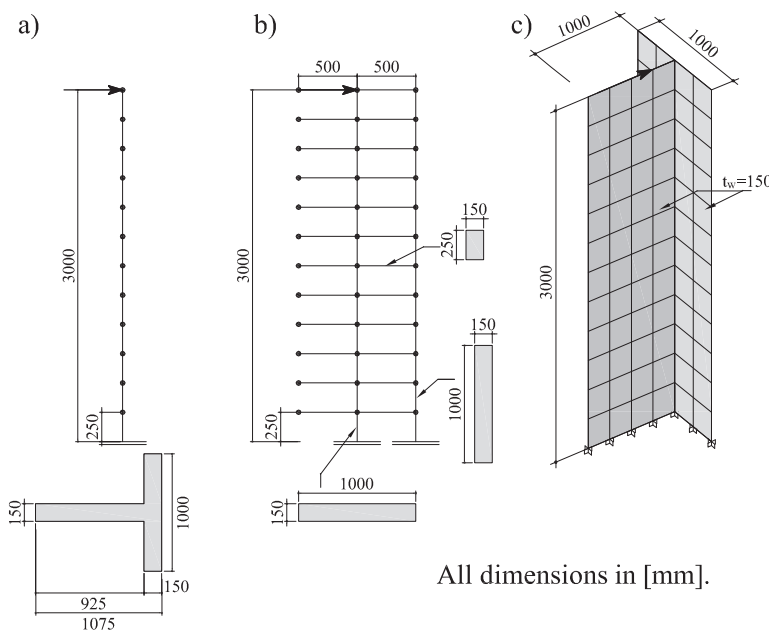


Figure 3 Models of T-shaped wall with elastic properties: Stick model (a), WCM (b) and shell element model (c).

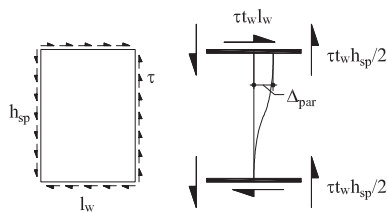


Figure 5 Wall section subjected to uniform shear along its edges and the corresponding wide-column element subjected to parasitic bending moment and artificial flexural deformations.

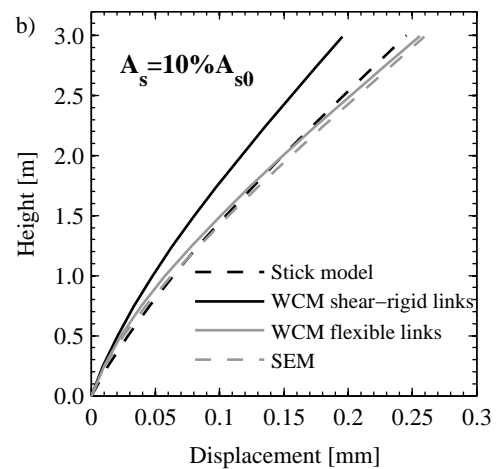
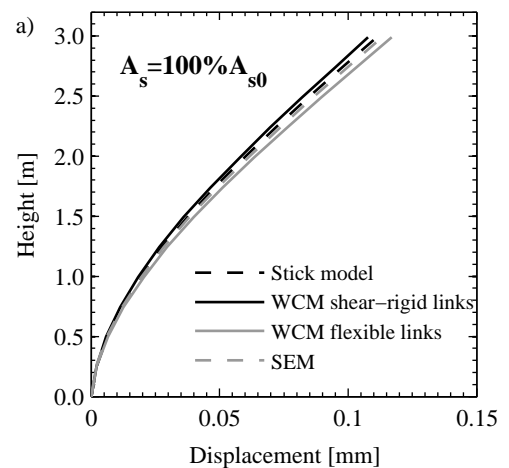


Figure 4 Deflected shapes of different elastic models of a T-shaped wall for the shear stiffness corresponding to an elastic uncracked section (a) and a reduced shear stiffness (b).

proposed where  $G$  is the shear modulus,  $h_{sp}$  the spacing of the horizontal links, and  $t_w$  the wall thickness. By assigning the links a torsional flexibility the section is no longer forced to remain plane. We suggest, however, that the links should also be assigned a shear flexibility to account for deformations due to the vertical shear stresses in the wall element. To demonstrate the necessity of a shear flexibility of the links the deflected shape of the following four different types of models are compared: (i) a stick model with a T-shaped section, (ii) a WCM where the links are modeled as rigid in shear, (iii) a WCM where the links are assigned a shear flexibility, and (iv) a shell element model (SEM). The vertical elements of the stick model and the WCMs have both shear and flexural flexibility; all models were analyzed with SAP2000 (CSI, 2006). The stick model and the SEM serve as a benchmark since they are expected to yield the correct shear stiffness. For a large shear stiffness ( $A_s=A_{s0}=0.8A_{gross}$ , Fig. 4a) the deflected shape of the WCM with shear rigid links is slightly stiffer than the stick model and the SEM while the WCM with shear flexible links is slightly softer. The latter is expected since the parasitic bending moments (Lew and Narov, 1983; Stafford Smith and Girgis, 1986) caused by lumping the continuous shear stresses along the wall edges into discrete shear forces in the links cause reverse bending of the vertical elements which have no physical meaning but introduce an artificial flexibility to the model (Fig. 5). If the shear stiffness is reduced to 10% of  $A_{s0}$  the difference between the two WCMs becomes more evident: The WCM with shear rigid links is clearly too stiff while the WCM with shear flexible links yields a deflected shape very similar to the ones of the stick model and the SEM. This comparison shows that the links in WCMs should not only be assigned a torsional flexibility but also a vertical shear flexibility; all other DoFs should be modeled as rigid. In the “reference model” of TUA which follows the modeling guidelines previously available in the literature (though they were mainly derived for models with elastic properties), the horizontal links were assigned a torsional stiffness  $GK$  only, while in the “updated model” the torsional stiffness was reduced to  $0.25GK$  to account for cracking and a shear flexibility was introduced.

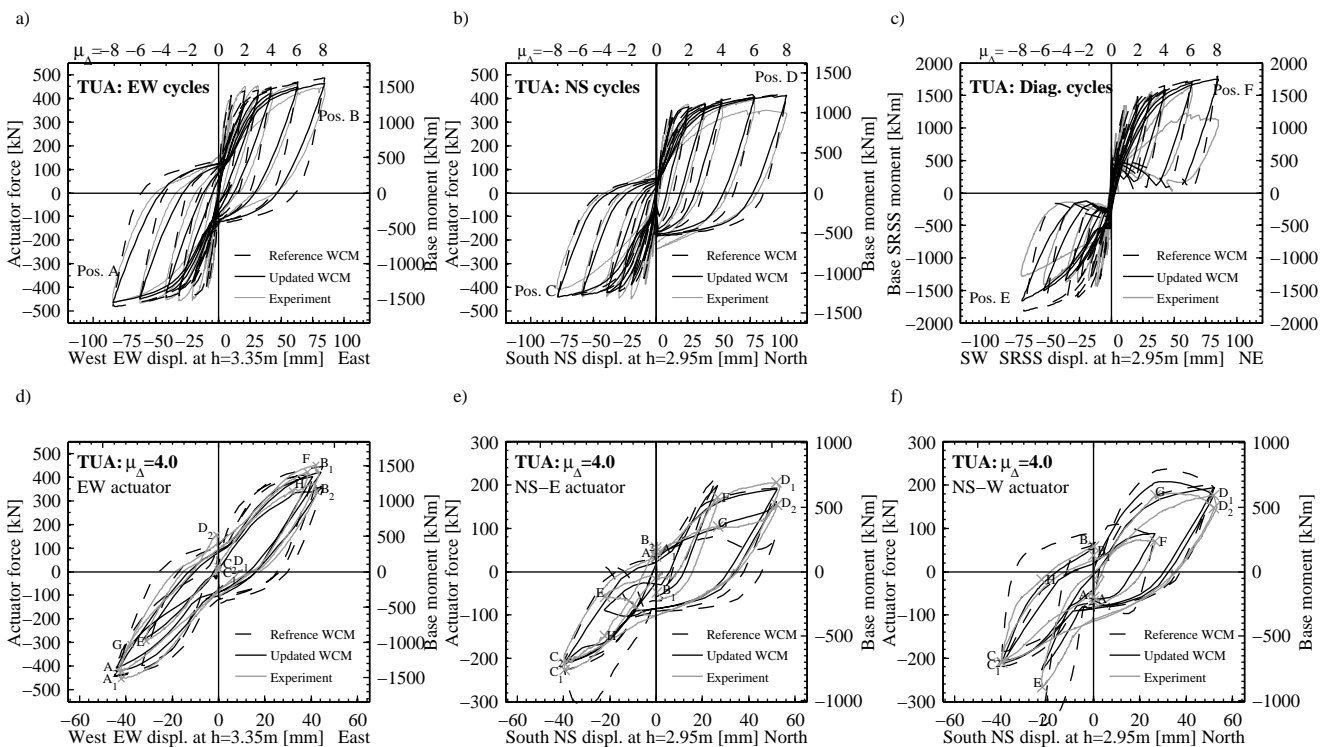


Figure 6 Comparison of the results obtained from the WCM models with state-of-the-art properties (“reference model”) and improved estimates of the shear stiffnesses (“updated model”) with the experimental results: Force-displacement hysteresis of TUA for the cycles in EW, NS and diagonal direction (a-c) and actuator forces during the cycles at  $\mu_{\Delta} = 4.0$  (d-f).

Figure 6 shows the hysteretic curves obtained for the “reference model” and the “updated model” in comparison to the experimentally determined curves. The top row of plots shows the hysteretic curves for the cycles parallel to the web (Fig. 6a), parallel to the flanges (Fig. 6b) and in diagonal direction (Fig. 6c) while the bottom row shows the three actuator forces during the cycles of  $\mu_{\Delta} = 4.0$  (Fig. 6d-f). The figure clearly shows that the “reference model” is too stiff when loading and unloading the structure leading, in particular for the diagonal direction, to an overestimation of the maximum forces reached during testing. On the contrary, the “updated model” matches the

experimental results rather well for  $\mu_{\Delta} \geq 4.0$ ; for cycles smaller than  $\mu_{\Delta} = 4.0$  the model is too soft because the shear stiffness of the wall was modeled as linear elastic corresponding to the shear stiffness at  $\mu_{\Delta} = 4.0$  (see previous paragraph). To demonstrate the effect on the shear stiffness on the force-displacement hysteresis obtained by the “updated model”, Fig. 7a shows their envelope curves for shear stiffnesses estimated at different displacement ductilities for the cycles in diagonal direction. The differences are in particular evident when loading to Position E. In Fig. 7b, the peak values from the WCMs with different shear stiffnesses are joined together to construct a composite envelope: The data point at  $\mu_{\Delta} = 1.0$  was computed from the WCM with a shear stiffness representative for  $\mu_{\Delta} = 1.0$ , the data point at  $\mu_{\Delta} = 2.0$  with a shear stiffness representative for  $\mu_{\Delta} = 2.0$ , etc.. The comparison with the experimental force-displacement hysteresis shows that this method allows to construct a good estimate of the envelope.

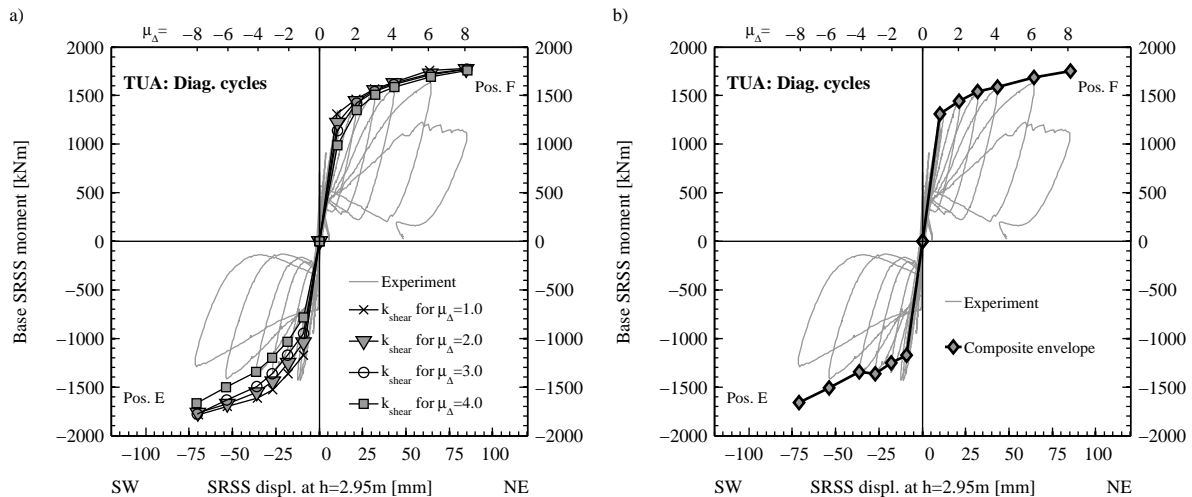


Figure 7 Comparison of the force-displacement envelopes for shear stiffness evaluated at different displacement ductilities for cycles in the diagonal direction: Individual envelopes (a) and composite envelope (b).

#### 4. MACRO-ELEMENT MODEL OF THE U-SHAPED WALLS USING THE PROGRAM “PERFORM”

The second modeling approach evaluated in this study made use of the macro elements implemented in the program “PERFORM 3D” (CSI, 2007). With this program shear walls can be either modeled with shear wall elements or with the general wall element. The “shear wall element” is a macro-element with 4-nodes and 24 degrees of freedom (DoFs). It is organized in two “layers” where each layer is assigned a specific load carrying mechanism: The first layer is modeled with a fiber section and accounts for the axial and flexural deformations parallel to the element axis while the second layer is the shear layer, i.e. an element subjected to uniform shear. This shear layer can be assigned elastic or inelastic properties but for the sake of simplicity it was only assigned elastic properties corresponding to 2.5% of the elastic uncracked shear stiffness. This corresponds approximately to the ratio derived from experimental evidence at  $\mu_{\Delta} = 4.0$ . All other deformation modes (e.g. out-of-plane bending) were assigned linear-elastic properties.

Figure 2c shows the PERFORM model of TUA. The chosen discretization was rather detailed to allow the modeling of every reinforcing bar separately; for design purposes it is common to choose a coarser discretization, e.g. only one element per wall and storey. However, this introduces additional approximations which might be acceptable for design but in the study here the objective was to sound the capabilities of this modeling approach with respect to the modeling of the inelastic behavior of non-rectangular walls subjected to bi-directional loading. The effects introduced by a coarser discretization should be investigated in a future study. The element formulation is such that the axial strain, shear strain and curvatures are constant over the height of an element and correspond effectively to the bending moment at midheight of the element. To model the strain demand at the base of the wall more realistically the length of the lowest element was therefore doubled and hence penetrating into the foundation (Fig. 2c).

The second macro-element in PERFORM suitable for the modeling of shear walls is the so called “general wall element”. Regarding the number of DoFs and the element formulation it is very similar to the “shear wall element”. However, it consists of 5 instead of 2 layers. In addition to the layers of the shear wall element, a layer with a fiber section with horizontal fibers and two layers which can model the diagonal compression strut actions for both diagonals are introduced. Figure 8 shows the comparison of the PERFORM model with “shear wall elements” (SW) and the PERFORM model with the “general wall element” (GW) to the experimental results in terms of the hysteresis curves (Fig. 8a-c) and the actuator forces during the cycles of  $\mu_A=4.0$ . The agreement between the numerical models and the experimental evidence is particularly good for the model with general wall elements. The model with shear wall elements is somewhat too stiff and also does not capture the distribution of the NS-force between the two flanges very well (Fig. 8e+f).

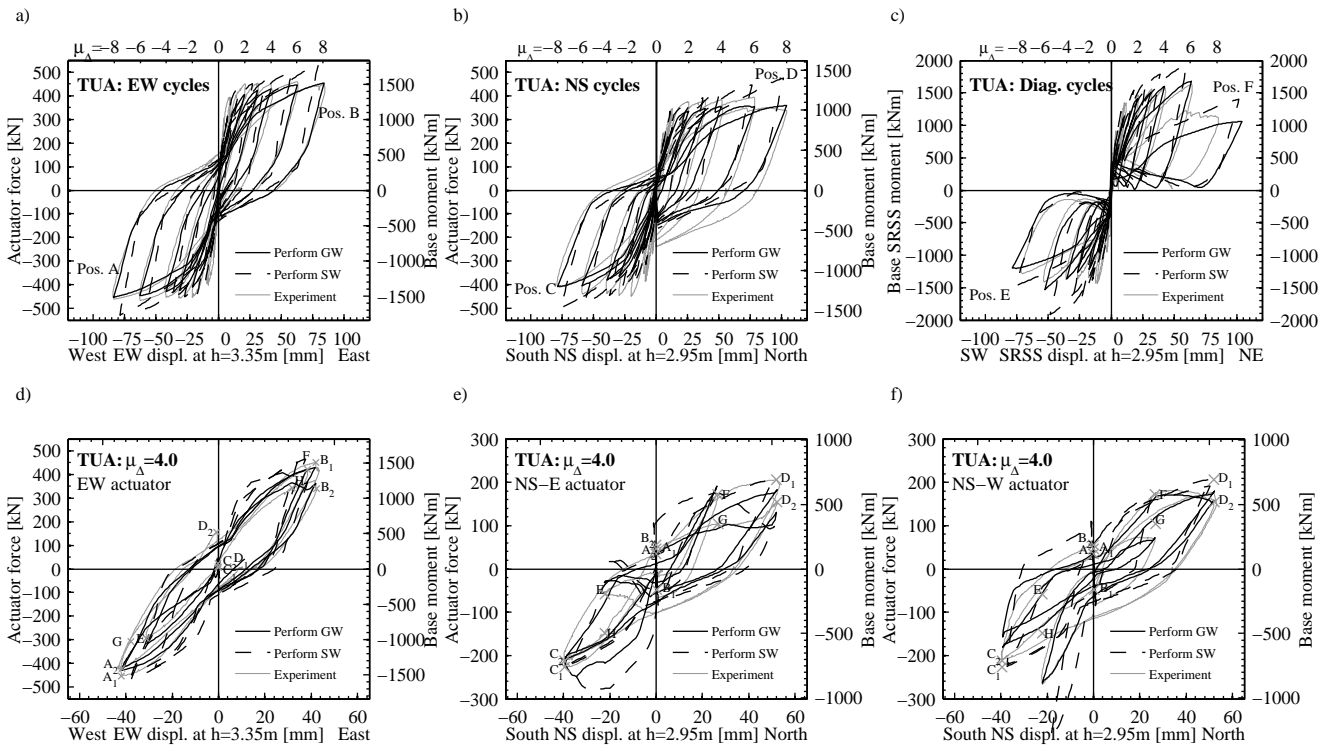


Figure 8 Comparison of the results obtained from the PERFORM models with the general wall element (GW) and the shear wall element (SW) with the experimental results: Force-displacement hysteresis of TUA for the cycles in EW, NS and diagonal direction (a-c), and actuator forces during the cycles at  $\mu_A=4.0$  (d-f).

## 5. CONCLUSIONS

The objective of this paper was to evaluate two relatively simple numerical models regarding their capability of modeling the inelastic response of U-shaped walls subjected to bi-directional loading. The two models were the wide-column model (WCM) and a macro-element model implemented into the structural analysis software “PERFORM 3D”. Both models are suitable for the analysis of entire buildings as well as isolated wall components and can therefore be used in engineering practice. The numerical results were compared against experimental evidence gained from quasi-static cyclic tests on U-shaped walls carried out at the ETH. The comparison of the numerical and experimental results in terms of different force-displacement hysteresses showed that a good estimate of the shear stiffness is crucial if one is not just solely interested in the force capacity of the wall but also in the hysteretic behavior. The analyses have also shown that the distribution of the force between the two flanges is particularly sensitive to the assumed shear stiffness. This finding holds for both the wide-column model and the PERFORM models. A novelty in the WCM was the introduction of a shear flexibility to the horizontal links which are typically modeled as rigid apart from the torsional DoF. By comparing the analysis results of elastic wide-column models to the results of stick models and shear element

models it could be shown that the shear-flexibility of the links is necessary to obtain the correct stiffness of the wall. The larger the contribution of the shear deformations to the total deformations the larger is the error if this shear flexibility is neglected.

## REFERENCES

- Avramidis, I.E. (1991). Zur Kritik des äquivalenten Rahmenmodells für Wandscheiben und Hochhauskerne (Criticism of the equivalent frame model for structural walls and cores in high-rise buildings). *Bautechnik* **68:8**, 275-285.
- Beyer, K., Dazio, A., and Priestley, M.J.N. (2008a). Quasi-Static Cyclic Tests of two U-shaped Reinforced Concrete Walls. *Journal of Earthquake Engineering*, in press.
- Beyer, K., Dazio, A., and Priestley, M.J.N. (2008b). Inelastic Wide-Column Models for U-Shaped Reinforced Concrete Walls. *Journal of Earthquake Engineering* **12:Sp1**, 1-33.
- CEN (1994). Eurocode 8: Design provisions for earthquake resistance of structures, Part 1: General rules, Part 1-1: Seismic actions and general requirements for structures; Part 1-2: General rules for buildings; Part 1-3: Specific rules for various materials and elements. ENV 1998-1-1, 1-2 and 1-3, European Committee for Standardization, Brussels, Belgium.
- Clough, R.W., King, I.P. and Wilson, E.L. (1964). Structural analysis of multistory buildings. *Journal of the Structural Division, ASCE* **90:ST3**, 19-34.
- CSI (2006). PERFORM 3D v4 – Nonlinear Analysis and Performance Assessment for 3D Structures. Computer and Structures, Inc., Berkeley, California.
- CSI (2007). SAP2000 v11.0.2 – Static and Dynamic Finite Element Analysis of Structures. Computer and Structures, Inc., Berkeley, California.
- Dazio, A. (2000). Entwurf und Bemessung von Tragwandgebäuden unter Erdbebeneinwirkung (Seismic design of buildings with structural walls). PhD-Thesis ETH No. 13739, Swiss Federal Institute of Technology, Zurich, Switzerland, available online: <http://e-collection.ethbib.ethz.ch/view/eth:23609>.
- Lew, I.P. and Narov, F. (1983). Three-dimensional equivalent frame analysis of shearwalls. *Concrete International* **5:10**, 25-30.
- MacLeod, I.A. and Hosny, H.M. (1977). Frame analysis of shear wall cores. *Journal of the Structural Division, ASCE* **103:ST10**, 2037-2047.
- Mazzoni, S., McKenna, F., Scott, M.H. and Fenves, G. L. et al. (2006). OpenSees Command Language Manual. OpenSees v1.7.3, University of California, Berkeley, USA.
- Oesterle, R.G., Aristizabal-Ochoa, J.D., Shiu, K.N., and Corley, W.G. (1984). Web Crushing of Reinforced Concrete Structural Walls. *ACI Journal* **81:3**, 231-241.
- Pégon, P., Plumier, C., Pinto, A., Molina, J., Gonzalez, P., Colombo, A., Tognoli, P., Hubert, O. and Tirelli, D. (2000). U-Shaped Walls: Description of the Experimental Set-Up. TMR-ICONS-TOPIC5, JRC Special Publication No.I.00.141, JRC Ispra, Italy.
- Reynouard, J.-M. and Fardis, M.N. (2001). Shear wall structures. CAFEEL-ECOEST/ICONS Thematic Report No. 5, LNEC (Laboratório Nacional de Engenharia Civil), Lisboa, Portugal.
- SeismoSoft (2007). SeismoStruct v4.0.3 – A computer program for static and dynamic nonlinear analysis of framed structures. Online, Available from URL (<http://www.seismosoft.com>), Messina, Italy.
- Stafford Smith, B. and Girgis, A. (1986). Deficiencies in the wide column analogy for shearwall core analysis. *Concrete International* **8:4**, 58-61.
- Vallenas, J.M., Bertrero, V.V. and Popov, E.P. (1979). Hysteretic Behavior of Reinforced Concrete Structural Walls. Report UBC/EERC-79/20, University of California, Berkeley, California, USA.